

## BASIC SCIENCE

## Quantitative Assessment and Interpretation of Vaginal Conditions



Vladimir Egorov, PhD,<sup>1</sup> Miles Murphy, MD,<sup>2</sup> Vincent Lucente, MD,<sup>2</sup> Heather van Raalte, MD,<sup>3</sup> Sonya Ephrain, MD,<sup>2</sup> Nina Bhatia, MD,<sup>3</sup> and Nouné Sarvazyan, PhD<sup>1</sup>

## ABSTRACT

**Introduction:** Few means exist to provide quantitative and reproducible assessment of vaginal conditions from biomechanical and functional standpoints.

**Aim:** To develop a new approach for quantitative biomechanical characterization of the vagina.

**Methods:** Vaginal tactile imaging (VTI) allows biomechanical assessment of soft tissue and function along the entire length of the anterior, posterior, and lateral vaginal walls. This can be done at rest, with applied vaginal deformation, and with pelvic muscle contraction.

**Results:** Data were analyzed for 42 subjects with normal pelvic floor support from an observational case-controlled clinical study. The average age was 52 years (range = 26–90 years). We introduced 8 VTI parameters to characterize vaginal conditions: (i) maximum resistance force to insertion (newtons), (ii) insertion work (millijoules), (iii) maximum stress-to-strain ratio (elasticity; kilopascals per millimeter), (iv) maximum pressure at rest (kilopascals), (v) anterior-posterior force at rest (newtons), (vi) left-right force at rest (newtons), (vii) maximum pressure at muscle contraction (kilopascals), and (viii) muscle contraction force (newtons). We observed low to moderate correlation of these parameters with subject age and no correlation with subject weight. 6 of 8 parameters demonstrated a *P* value less than .05 for 2 subject subsamples divided by age ( $\leq 52$  vs  $> 52$  years), which means 6 VTI parameters change with age.

**Conclusions:** VTI allows biomechanical and functional characterization of the vaginal conditions that can be used for (i) understanding “normal” vaginal conditions, (ii) quantification of the deviation from normality, (iii) personalized treatment (radiofrequency, laser, or plastic surgery), and (iv) assessment of the applied treatment outcome. **Egorov V, Murphy M, Lucente V, et al. Quantitative Assessment and Interpretation of Vaginal Conditions. Sex Med 2018;6:39–48.**

Copyright © 2017, The Authors. Published by Elsevier Inc. on behalf of the International Society for Sexual Medicine. This is an open access article under the CC BY-NC-ND license (<http://creativecommons.org/licenses/by-nc-nd/4.0/>).

**Key Words:** Vaginal Conditions; Vaginal Force; Vaginal Work; Vaginal Pressure; Vaginal Elasticity; Tactile Imaging

## INTRODUCTION

Increasingly, radiofrequency and laser treatment technologies and plastic, esthetic, or cosmetic procedures are being used for vaginal modification. However, no reliable tools and techniques exist for objective assessment of vaginal conditions before and after the applied treatment. Clinicians who work with women

interested in changing the vaginal properties or functions of their genitalia inevitably come to understand the importance of objective anatomic, biomechanical, and functional measures for vaginal characterization to distinguish normal from abnormal conditions.<sup>1–4</sup>

Vaginal tactile imaging (VTI) allows for acquisition of bilateral pressure patterns along the entire length of the vagina.<sup>5</sup> This opens up new possibilities for characterization of the vagina and its functional properties.

The VTI approach resembles soft tissue palpation, which has been the most prevalent and successful medical diagnostic technique for accessible human organs and the musculoskeletal system, including malignant tumors, tissue inflammation, and atrophy.<sup>6,7</sup> 2 critical factors explain this technique: (i) detection of a mechanical heterogeneity by manual palpation is based exclusively on sensing variations of the Young modulus (*E*) of

Received April 10, 2017. Accepted August 23, 2017.

<sup>1</sup>Artann Laboratories, Trenton, NJ, USA;

<sup>2</sup>The Institute for Female Pelvic Medicine & Reconstructive Surgery, Allentown, PA, USA;

<sup>3</sup>Princeton Urogynecology, Princeton, NJ, USA

Copyright © 2017, The Authors. Published by Elsevier Inc. on behalf of the International Society for Sexual Medicine. This is an open access article under the CC BY-NC-ND license (<http://creativecommons.org/licenses/by-nc-nd/4.0/>).

<https://doi.org/10.1016/j.esxm.2017.08.002>

tissue and (ii) the elasticity modulus varies greatly (several times higher than its normal state) during the development of pathologic or diseased conditions in the soft tissues.<sup>8,9</sup> The key terms related to soft tissue elasticity and tactile imaging require additional explanation for understanding.

In mechanics, elasticity is the ability of a material to resist applied stress and to return to its original shape when the stress is removed. Elastic moduli characterize the ability to resist the applied stress as an intrinsic property of the specific material.<sup>10–12</sup> In the case of 1-dimensional deformation of a uniform object, the stress-to-strain ratio is the Young modulus (stress/strain =  $[N/m^2]/[m/m] = Pa$ ; Hooke's law). Many materials, including human soft tissues, noticeably deviate from Hooke's law well before their elastic limits (tissue break) are reached. However, the stress-to-strain ratio directly characterizes soft tissue elasticity.

Pressure response patterns, when measured with a pressure sensor array by applying a probe to the surface of a soft tissue object, allow acquisition of the stress data. If we know the exact displacement coordinates (strain) of every pressure sensor during tissue deformation, we can map the pressure response data in this coordinate continuum to generate stress-strain or tactile images.

Tactile imaging is a medical imaging modality translating the sense of touch into a digital image. The tactile image is a function of  $P(x,y,z)$ , where  $P$  is the pressure on the soft tissue surface under applied deformation and  $x$ ,  $y$ , and  $z$  are the coordinates where pressure  $P$  is measured.<sup>13</sup> The tactile image is a pressure map on which the direction of tissue deformation must be specified. The probe with a pressure sensor array mounted on its face acts similarly to human fingers during clinical examination in deforming soft tissue by the probe and detecting resulting changes in the pressure pattern on the surface. The sensor head is moved over the surface of the tissue to be studied, and the pressure response is evaluated at multiple locations along the tissue under study. The results are used to generate 2- or 3-dimensional images showing the pressure distribution over the area of tissue under study.

In general, an inverse problem solution for the 3-dimensional tactile image  $P(x,y,z)$  would allow reconstruction of the tissue elasticity distribution as a function of the coordinates  $x$ ,  $y$ , and  $z$ . Unfortunately, the inverse problem solution is hardly possible for complex organ and tissue structures because it is a non-linear and ill-posed problem. However, tactile imaging displays tissue or organ anatomy and elasticity distribution because it keeps the stress-strain relation for deformed tissue. It appears that the 3-dimensional tactile image can be transformed into an elasticity image with the use of a linear transformation for a region of interest. In general, that means the spatial gradients  $\partial P(x,y,z)/\partial x$ ,  $\partial P(x,y,z)/\partial y$ , and  $\partial P(x,y,z)/\partial z$  can be used in practice for a quantitative assessment of soft tissue elasticity despite structural and anatomic variations.<sup>13</sup>

Functional tactile imaging is a variation of tactile imaging that translates muscle activity into a dynamic pressure pattern  $P(x,y,t)$  for an area of interest, where  $t$  is time and  $x$  and  $y$  are coordinates where pressure  $P$  is measured. Muscle activity to be studied can include a voluntary contraction (eg, a pelvic floor squeeze), an involuntary reflex contraction (eg, due to a cough), an involuntary relaxation, or a Valsalva (veering down) maneuver.<sup>14</sup> Functional tactile imaging is similar to the high-definition manometry used for muscle contraction studies along the gastrointestinal tract.

Biomechanical and functional assessment of the vaginal conditions and then tailoring treatment and its outcome assessment compose the logical route to improved satisfaction of patients.

The aim of this research was to develop a patient-specific approach for diagnostic characterization of vaginal biomechanical and functional components. This approach is based on the current understanding of female pelvic floor functional anatomy<sup>15–17</sup> and interpretation of clinical results with VTI.

## METHODS

### Population Description

We analyzed 42 subjects with normal pelvic floor conditions (no pelvic organ prolapse) from a completed observational case-controlled clinical study in 2014 to 2015 (clinical trial identifier NCT02294383 at <http://clinicaltrials.gov>). The average subject age was 52 years (range = 26–90 years). Age comparisons (>52 vs <52 years) were based on the timing of menopausal transition (average age = 51 years). The clinical study with VTI was approved by the local institutional review board, and all women gave written informed consent. The study was performed in compliance with the Health Insurance Portability and Accountability Act. VTI images were obtained and recorded at the time of scheduled routine gynecologic visits.

Total study workflow consisted of the following steps: (i) recruiting women who routinely undergo vaginal examination as a part of their diagnostic treatment of concerned areas; (ii) acquisition of clinical diagnostic information related to the studied cases by standard clinical means; (iii) performing a VTI examination; and (iv) review and analysis of acquired VTI data.

### Patient Position and VTI Examination Procedure

VTI is performed on a patient in the dorsal lithotomy position with an empty bladder and rectum. The full VTI examination takes 2 to 3 minutes to complete. The VTI probe is calibrated before every clinical application. [Figure 1](#) shows VTI probe placement into the vagina during the patient examination (data acquisition). The reported VTI study consists of 3 independent tests: (i) probe insertion, (ii) probe rotation, and (iii) voluntary muscle contractions for anterior vs posterior.

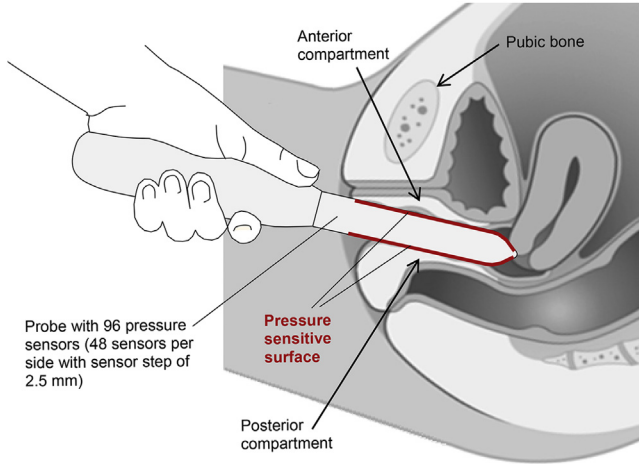


Figure 1. Vaginal tactile imaging probe during examination.

### Vaginal Tactile Imager

VTI allows the acquisition of pressures applied to the vaginal walls and the probe location to visualize vaginal and pelvic floor support structures and to record pelvic floor muscle contractions. The VTI software provides visualization, analysis, information, and reporting tools. The acquired data and analysis information can be used for quantitative assessment of the vaginal and pelvic floor conditions. The VTI device consists of the vaginal probe (Figure 1) and a movable computer display cart (not shown). The VTI probe is equipped with 96 pressure (tactile) sensors positioned every 2.5 mm along both sides of the probe, an orientation sensor, and temperature sensors with micro-heaters.

During the patient examination procedure, data are sampled from the probe sensors and displayed on the VTI computer display in real time. The probe surfaces that contact the vaginal walls are preheated to human body temperature. A lubricating jelly is used for patient comfort and to provide reproducible boundary-contact conditions with deformed vaginal tissue; these conditions are classified as slip boundary conditions. The VTI data analyses in this article reflect single trials. Intra- and inter-observer reproducibility of VTI was explored in a prior study under similar conditions.<sup>18</sup>

The tactile probe measures an applied pressure, but not force. This probe allows (i) compression of vaginal tissues in the orthogonal direction to the tissue surface (vaginal walls) during probe insertion (test 1), (ii) vaginal wall deformation and pressure pattern acquisition during probe rotation (test 2), and (iii) acquisition of pressure patterns for pelvic muscle contraction (test 3) along the entire vagina. The probe maneuvers allow accumulation of multiple pressure patterns from the tissue surface to compose an integrated tactile image for each test area using image composition algorithms.<sup>19</sup> The device is intended for use by physicians, surgeons, and medically trained personnel. Previous clinical results with VTI have been reported.<sup>20–26</sup> This device has been approved by the Food and Drug Administration for the characterization of vaginal conditions.

### VTI Parameters

We propose 8 new VTI parameters to characterize vaginal conditions:

#### Maximum Resistance Force to Insertion (Newtons)

During probe insertion, we can calculate the force applied to the probe  $F_1(x)$  along the vaginal canal (vaginal resistance) from the measurement of pressure distribution  $P_t$  on the tip under angle  $\alpha$  of the probe and its tissue contact area  $A_t$  (Figure 2A). Maximum insertion force  $F_{lmax}$ , expressed in newtons, is calculated for probe insertion until the probe meets the cervix. Factor  $\cos(\alpha)$  in equation (1) is used to count only the force projection along the vaginal canal.

$$F_1(x) = \cos(\alpha) \times \sum_{\text{probe tip}} (P_t \times A_t) \quad (1)$$

$$F_{lmax} = \max_{x=0 \dots \text{cervix}} (F_1[x]) \quad (2)$$

#### Insertion Work (Millijoules)

During probe insertion, we can calculate the work  $W_1$  completed by an operator. The amount of this work done is determined by probe force  $F_1(x)$  multiplied by probe displacement  $\Delta x$  during probe insertion into the vagina. Its units are joules ( $J = N \times m$ ) or millijoules.

$$W_1 = \sum_{x=0 \dots \text{cervix}} (F_1[x] \times \Delta x) \quad (3)$$

#### Maximum Stress-to-Strain Ratio (Elasticity; Kilopascals per Millimeter)

We can calculate the gradients in the acquired tactile image (Figure 2) for every probe position during probe insertion along the vaginal canal for the anterior and posterior compartments ( $G_{la}[x] = \partial P / \partial y$ ) and the posterior compartments ( $G_{lp}[x] = -\partial P / \partial y$ ). We defined maximum the stress-to-strain ratio according to expression (4) as kilopascals per millimeter. This parameter characterizes maximum tissue elasticity along the vagina.

$$G_{lmax} = (\max_{x=0 \dots \text{cervix}} [G_{la}\{x\}] + \max_{x=0 \dots \text{cervix}} [G_{lp}\{x\}]) / 2 \quad (4)$$

#### Maximum Intravaginal Pressure at Rest (Kilopascals)

During probe rotation through an angle  $\Omega = 0 \dots 360^\circ$  inside the vagina, we can define the maximum pressure in the vagina (Figure 3) as  $P_{rmax}$ .

$$P_{rmax} = \max_{x=0 \dots \text{cervix}} (P[x, \Omega]) \quad (5)$$

#### Anterior vs Posterior Force at Rest (Newtons)

This  $F_{ap}$  force is calculated as a cumulative force applied to all 96 pressure sensors when the tactile sensitive area comes in

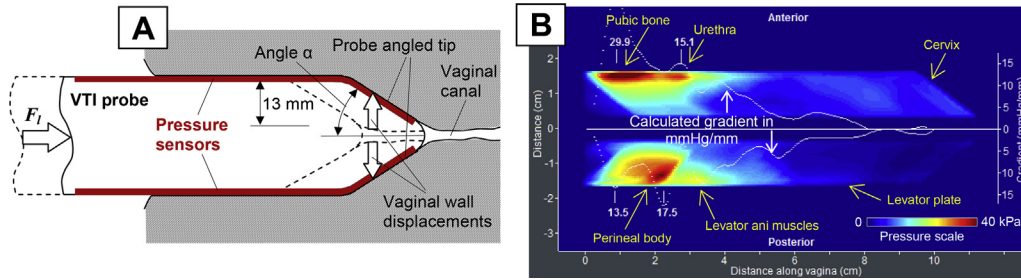


**Figure 2.** Panel A shows VTI probe insertion to deform vaginal walls by a definitive manner. Panel B shows a tactile image with calculated gradients for VTI probe insertion for a 37-year-old woman with normal pelvic floor conditions.  $F_I$  = force applied to insertion probe; VTI = vaginal tactile imaging

contact with the anterior force produced,  $F_a$ , and its posterior equivalent  $F_p$  along the entire vagina at rest.

$$F_{ap} = \sum_{x=0 \dots cervix} (F_a[x] + F_p[x]) \tag{6}$$

**Left vs Right Force at Rest (Newtons)**

This  $F_{lr}$  force is calculated as a cumulative force applied to all 96 pressure sensors when the tactile sensitive area comes in contact with the force produced by the left side,  $F_l$ , and the force produced by the right side,  $F_r$ , of the vagina along the entire vagina at rest.

$$F_{lr} = \sum_{x=0 \dots cervix} (F_l[x] + F_r[x]) \tag{7}$$

**Maximum Intravaginal Pressure at Pelvic Muscle Contraction (Kilopascals)**

During voluntary pelvic muscle contraction, we can define the maximum pressure in the vagina as  $P_{cmax}$  for acquired intravaginal pressure distribution  $P_c(x)$  along the entire anterior and posterior compartments.

$$P_{cmax} = \max_{x=0 \dots cervix} (P_c[x]) \tag{8}$$

**Muscle Contraction Force (Newtons)**

This  $F_c$  force is calculated as a cumulative force increase acting on all 96 pressure sensors during voluntary pelvic floor muscle contraction, when the tactile sensitive area comes in contact with

the anterior force produced,  $F_{ca}$ , and its posterior equivalent,  $F_{cp}$ , along entire vagina. The forces at rest  $F_a$  and  $F_p$  are subtracted from the forces at maximum contraction values.

$$F_c = \sum_{x=0 \dots cervix} (F_{ca}[x] + F_{cp}[x]) - \sum_{x=0 \dots cervix} (F_a[x] + F_p[x]) \tag{9}$$

**Correlations**

Correlation coefficients (R) were calculated as the sample Pearson correlation coefficient defined by a ratio of sample covariances to variances. A t-test was performed to determine whether 2 samples could have the same mean when the SDs are unknown but assumed equal. The age comparisons (>52 vs <52 years) were based on the average timing of menopausal transition to make a gross comparison.

We considered the applicability of Bonferroni corrections. With familywise multiplicity correction, the test-specific significance level depends on how the family is defined. For example, if all 8 independent hypotheses were included in the test family, then the Bonferroni corrected significance level would be a P value equal to .05/8 equal to .00625 instead of .05.<sup>27</sup> However, the standard Bonferroni method assumes that each of the 8 comparison tests is an independent hypothesis, and this is clearly not the case (eg, maximum pressure with muscle contraction and muscle contraction force are mutually influenced by the same muscles; maximum resistance to force, insertion work, and elasticity reflect tissue resistance; given the shape of the vagina,

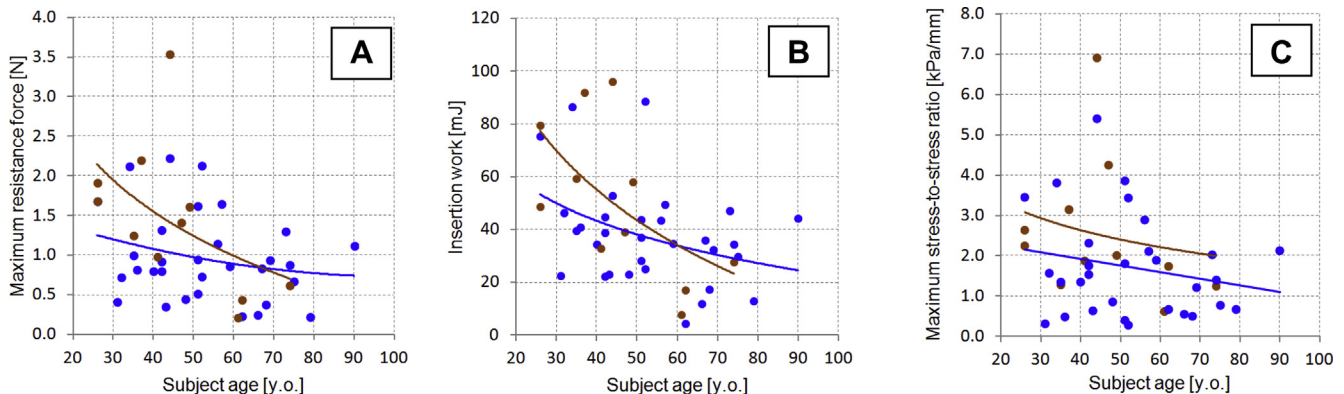


**Figure 3.** Panels A to C show vaginal tactile imaging parameters 1 to 3, respectively, vs subject's age. Blue dots + trend lines = parous; brown dots + trend lines = nulliparous.

resting anterior-posterior and left-right forces are interdependent depending on where the measurement is collected). It seems 3 comparisons are appropriate ( $P = .05/3 = 0.017$ ). That means that findings with a  $P$  value greater than .017 must be interpreted as rejection of the universal null hypothesis.<sup>28</sup> However, in the present research, we assessed each VTI parameter separately.

## RESULTS

### Test 1: Probe Insertion

The vaginal probe is designed to deform the vaginal walls in the orthogonal direction from the vaginal channel during probe insertion (Figure 2A). The linear motion of the probe is translated into vaginal tissue deformation in a definitive manner and the pressure sensors on the angled probe tip measure the tactile feedback from the vaginal walls for 13 mm deformation per side (Figure 2A).

During clinical examination, before probe insertion, the anterior and posterior vaginal walls are almost in contact with each other at patient-relaxed conditions in the dorsal position. The internal pressure along the vaginal channel is close to 0. During VTI probe insertion, the probe finds equilibrium from 2 opposite sides (anterior vs posterior) and an operator allows the probe to follow the insertion angle of least resistance along the vaginal canal. Probe insertion can be completed in less than 10 seconds and the operator observes an acquired tactile image in real time.

Figure 2B shows the test 1 clinical result for normal pelvic floor conditions. Locations of specific pelvic floor structures are marked on this image. The tactile image for this test characterizes the vaginal tissue elasticity behind the vaginal walls at a distance comparable to the value of the tissue deformation (0–10 mm). The vaginal wall seems significantly softer than the structures we observe deeper beneath the wall. Specifically, from left to right in the anterior vaginal compartment, we see responses from the pubic bone, urethra, and cervix.<sup>15–17</sup> In the posterior compartment, from left to right, the responses are observed from a perineal body; levator ani muscles and levator plate are present (Figure 2B). White dotted lines in Figure 2B are spatial pressure gradients calculated from the center of the vaginal channel to the anterior and posterior directions.

The tactile image shown in Figure 2B demonstrates a relatively high-pressure gradient (up to 17.5 mm Hg/mm) for the posterior compartment vs 29.9 mm Hg/mm for the left image shown in Figure 2B. These gradient values can be interpreted as vaginal tissue elasticity within 0 to 10 mm from the vaginal walls. Changes in vaginal wall tissue, such as surgical scar tissue, vaginal atrophy, and changes after laser treatment, can be quantified and observed.<sup>20</sup> An anatomic factor also can contribute to this image; for example, an enlarged vaginal hiatus will show low-pressure gradient at the entrance (the 1st 2–3 cm). However, as the VTI probe moves deeper into the vagina, the probe pushes apart the anterior and posterior vaginal walls simultaneously and records the pressure response from their displacements. An

important aspect is that the tactile images presented in Figure 2 are composed of the local vaginal wall deformations, not the entire vagina at the same time. Only acquired dynamic (not static) pressure data from the probe tip sensors (angled probe tip zones in Figure 1) contribute to the images of test 1. These images become more sensitive and informative when tactile (stress-strain) data for opposite vaginal walls are shown during their deformation along the vagina. A relatively weak signal from the cervix shown in Figure 2B can characterize weak (laxity) conditions of uterosacral and cardinal ligaments.

Test 1 allows, as defined in the Methods section, the calculation of:

1. Maximum resistance force to insertion  $F_{\text{Imax}}$  (newtons; Figure 3A)
2. Insertion work  $W_1$  (millijoules; Figure 3B)
3. Maximum stress-to-strain ratio  $G_{\text{Imax}}$  (kilopascals per millimeter; elasticity; Figure 3C)

Figures 3A to 3C show the distributions of these parameters vs age among the studied subjects. Trend lines are presented separately for nulliparous and parous subjects.

### Test 2: Probe Rotation

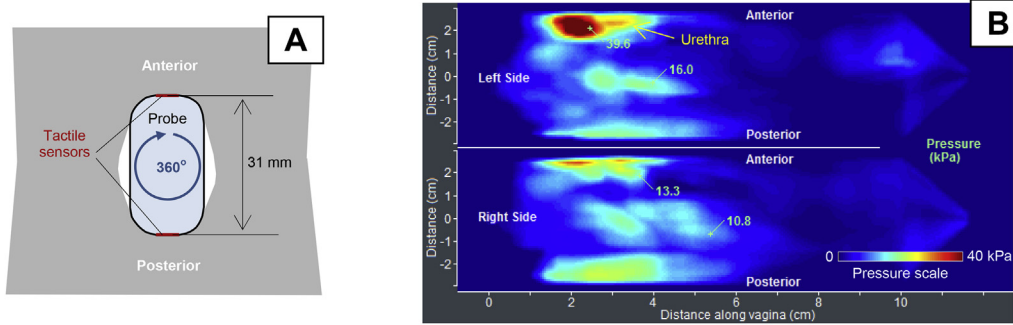
The vaginal probe, when rotated by 360° as shown in Figure 4A, allows acquisition of circumferential tactile feedback from the vaginal walls. The probe has an orientation sensor to measure its rotational angle; therefore, the pressure feedback can be mapped along the rotation angle for the left and right sides (Figure 4B). The VTI probe should be slowly rotated to control image quality on the VTI computer display. Each of the vaginal walls is deformed up to 7 mm during VTI probe rotation.

Figure 4B presents the clinical case for normal pelvic floor support (no prolapse conditions) with strong pressure feedback at the center of the left and right sides of the distal part ( $P = 133\text{--}168$  mm Hg). Any local pressure peaks at the vaginal sides can be interpreted as stiff irregularities or lumps on the vaginal wall or behind it at a depth of 0 to 7 mm. Vaginal width definitely contributes to the tactile feedback at the center of the left and right sides when the probe is oriented horizontally; thus, the right side is exactly imaged vs the left side. Asymmetry in pressure patterns on 1 side vs another side conveys information about asymmetric pelvic floor structures behind the vaginal walls.

Test 2 allows, as defined in the Methods section, the calculation of:

1. Maximum intravaginal pressure at rest (kilopascals; Figure 5A)
2. Anterior vs posterior force at rest (newtons; Figure 5B)
3. Left vs right force at rest (newtons; Figure 5C)

Figures 5A to 5C show the distributions of these parameters vs age among the studied subjects. Trend lines are presented separately for nulliparous and parous subjects.



**Figure 4.** Panel A shows a vaginal tactile imaging probe at 360° rotation at test 2. Panel B shows circumferential tactile image for a 49-year-old woman with normal pelvic floor support.

**Tests 3: Voluntary Muscle Contraction**

Figure 6 shows VTI data for a patient with normal pelvic floor support during voluntary pelvic floor muscle contractions.

This case displays 3 posterior peaks (Figure 6D, E) at pelvic muscle contractions. Based on the functional anatomy of the female pelvic floor, we can conclude that these peaks are produced by puboperineal, puborectal, and pubovaginal muscles.<sup>15–17</sup> Their muscle strength is estimated as the pressure increase during muscle contraction (Figure 6D). In the anterior compartment, the pressure response from the urethra is detectable (Figure 6A). A “muscle vibration” or oscillation of pressure for the puboperineal muscle with a period of approximately 0.5 second is observed in Figure 6C at its contraction. Figure 6F shows an example of the puboperineal-pubovaginal muscle desynchronization in part (not full synchronization at contraction); the pubovaginal muscle begins to contract approximately 0.3 second before the puboperineal muscle contracts.

Test 3 allows, as defined in the Methods section, the calculation of:

1. Maximum intravaginal pressure at pelvic muscle contraction (kilopascals; Figure 6A, B)
2. Muscle contraction force (newtons; as integral under pressure curves in Figures 6A, D)

Figures 7A and 7B show the distributions of these parameters vs age among the studied subjects. Trend lines are presented separately for nulliparous and parous subjects.

Table 1 presents the basic characteristics of the VTI parameters: Pearson correlation coefficients (R) with subject’s age and weight and t-tests and P values for the 2 groups subdivided by subject age and weight.

**DISCUSSION**

The results of this study demonstrated that the proposed approach allows acquisition of a set of biomechanical parameters characterizing the vagina. This set includes 8 VTI parameters: (i) maximum resistance force to insertion (newtons), (ii) insertion work (millijoules), (iii) maximum stress-to-strain ratio (tissue elasticity; kilopascals per millimeter), (iv) maximum pressure at rest (kilopascals), (v) anterior-posterior force at rest (newtons), (vi) left-right force at rest (newtons), (vii) maximum pressure at muscle contraction (kilopascals), and (viii) muscle contraction force (newtons). We observe significant variance (SDs) for the VTI parameters among the analyzed data sample (Table 1). This variance seems natural and is due to variations in anatomic and muscle (function) conditions. This variance is clearly beyond the VTI intra- and inter-operator reproducibility, which was

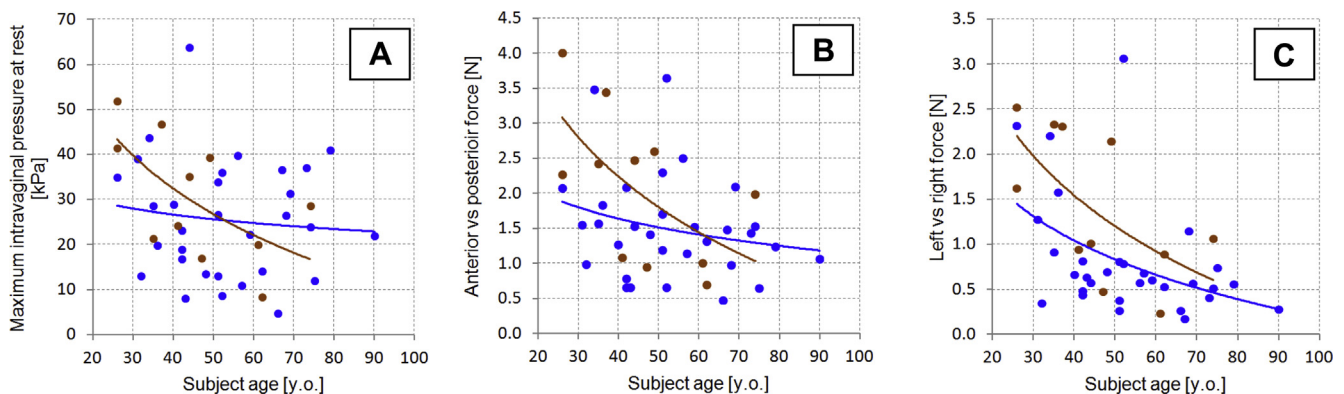


**Figure 5.** Panels A to C show vaginal tactile imaging parameters 4 to 6, respectively, vs subject’s age. Blue dots + trend lines = parous; brown dots + trend lines = nulliparous.

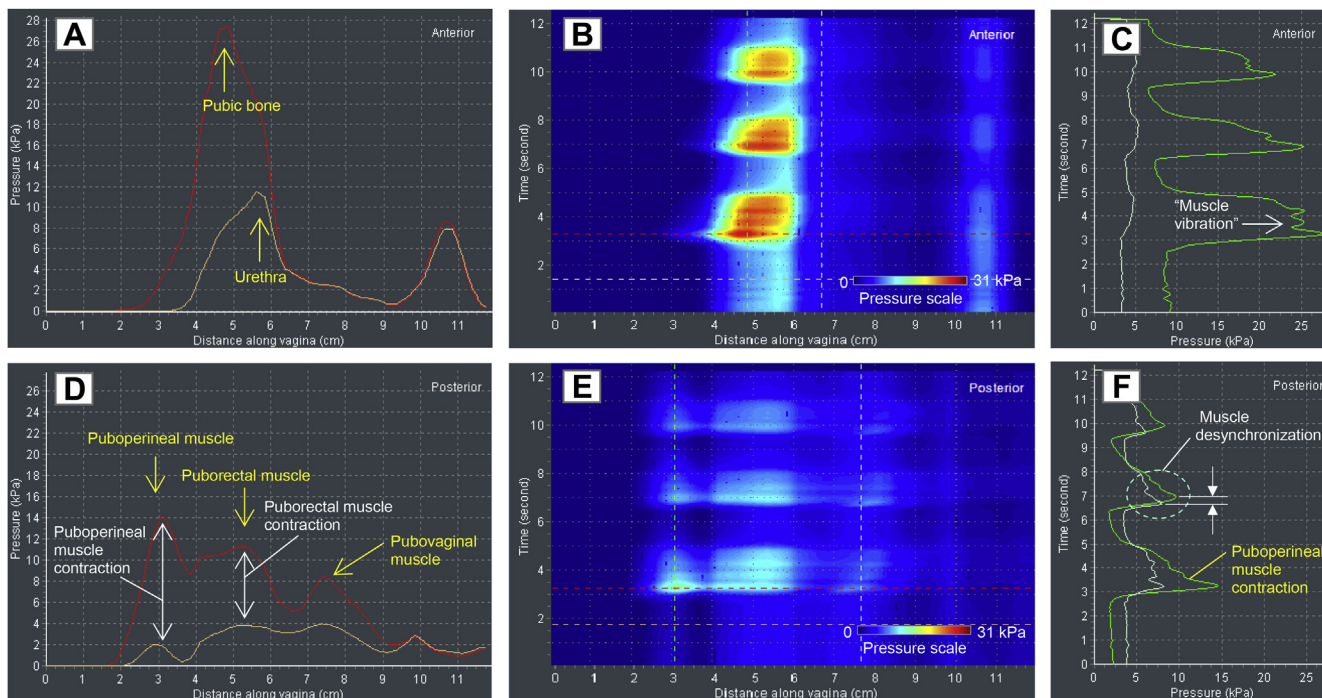


Figure 6. Panels A to F shows test 3 (voluntary muscle contraction) results for a 62-year-old patient with normal pelvic floor support.

estimated within 11.2% to 12.0% of limits of agreement, based on Bland-Altman plots with 95% limits, and within 0.80 to 0.92 of intraclass correlation coefficients in the clinical VTI reproducibility study.<sup>18</sup> Several explanations are plausible for this degree of variance, including parity, menopausal status, phase of menstrual cycle, tobacco use, other connective tissue conditions, or use of vaginal estrogen. Factors beyond weight and age were not evaluated in this study.

We observed low to moderate correlation of these parameters with subject age (from  $-0.26$  to  $-0.54$ ). 6 of 8 parameters

demonstrated a  $P$  value less than or equal to .05 for 2 subject subsamples divided by age ( $\leq 52$  vs  $>52$  years old), which means 6 VTI parameters change with age. Figures 3A to 3C demonstrate a general age-dependence of vaginal tissue properties; they also show that, after the menopausal transition, the variability of these measures appears to noticeably decrease. Correlation with menstrual cycle timing in the premenopausal patient would be a valuable investigation for future study and could explain the widened variance. The mean values for the age subgroups are listed in Table 1. We found a limited number of in vivo research publications about the changing of vaginal tissue elasticity with

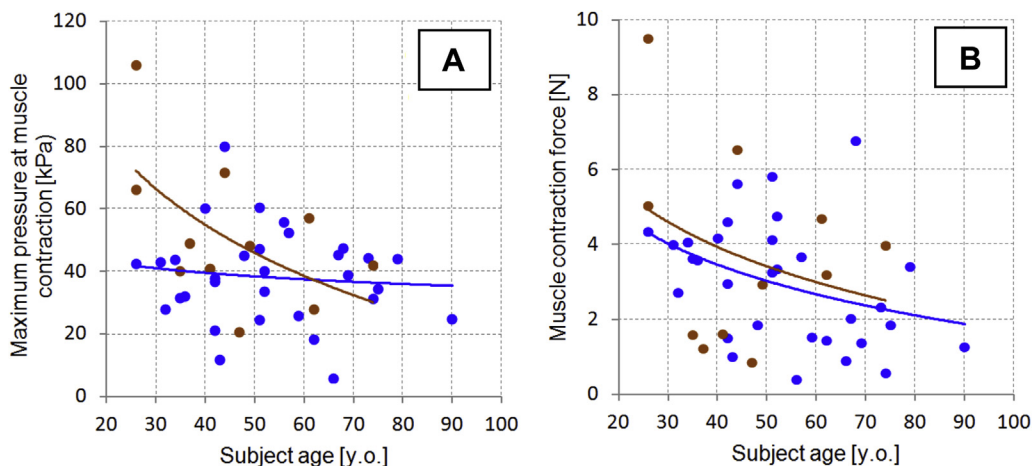


Figure 7. Panel A shows vaginal tactile imaging parameter 7 vs subject's age. Panel B shows vaginal tactile imaging parameter 8 vs subject's age. Blue dots + trend lines = parous; brown dots + trend lines = nulliparous.

**Table 1.** Studied sample characteristics and vaginal tactile imaging parameters

	Age (y)	Weight (lb)	Resistance (N)	Work (mJ)	Stress to strain (kPa/mm)	Pressure at rest (kPa)	Anterior-posterior force (N)	Left-right force (N)	Contraction pressure (kPa)	Contraction force (N)
Mean	52.7	152.6	1.09	41.3	1.94	26.8	1.66	0.98	41.8	3.20
SD	16.1	26.7	0.70	22.7	1.42	13.3	0.87	0.74	18.4	1.94
Minimum	26	110	0.21	4.5	0.28	4.7	0.47	0.18	5.9	0.39
Maximum	90	200	3.54	96.3	6.93	63.8	4.00	3.07	106.0	9.52
Correlation (R) with age	—	—	-0.36	-0.48	-0.26	-0.28	-0.40	-0.54	-0.32	-0.36
t-test ( $\leq 52$ vs $> 52$ y old; <i>P</i> value)	—	—	0.007	0.002	0.05	0.23	0.04	0.005	0.20	0.05
Correlation (R) with weight	—	—	-0.12	-0.10	-0.19	-0.24	-0.05	0.05	-0.05	-0.06
t-test ( $\leq 152$ vs $> 152$ lb; <i>P</i> value)	—	—	0.99	0.91	0.64	0.37	0.94	0.74	0.53	0.38
Mean (nulliparous)	—	—	1.44	50.9	2.55	30.4	2.08	1.42	51.7	3.75
Mean (parous)	—	—	1.01	37.8	1.72	25.6	1.51	0.82	38.2	3.00
t-test (nulliparous vs parous; <i>P</i> value)	—	—	0.05	0.10	0.10	0.30	0.06	0.02	0.04	0.27

the age.<sup>29–31</sup> In general, our findings fit with previous observations of vaginal tissue properties with age. Previously, we found that in the midposterior region of the vagina, the average values of the Young modulus decreased with age from  $13.1 \pm 7.8$  to  $6.1 \pm 3.0$  kPa; in apical posterior compartments, the average value of the Young modulus was  $13.2 \pm 3.1$  kPa for a 28- to 35-year-old group and  $3.0 \pm 1.5$  kPa for a 76- to 90-year-old group.<sup>13</sup> In the present research for normal pelvic floor conditions, we observed low to moderate correlation of these parameters with subject age (from  $-0.26$  to  $-0.54$ ).

We found no correlation with subject weight (from 0.05 to  $-0.24$ ). None of the 8 VTI parameters demonstrated a *P* value less than .05 for 2 subject subsamples divided by weight ( $\leq 152$  vs  $> 152$  lb), which means the VTI parameters do not change with weight. The weight subgroups did not exhibit significantly different mean values for the analyzed VTI parameters.

To examine the effect of parity, we separated nulliparous from parous subjects within the acquired dataset. Vaginal birth seems to affect VTI parameters 1 (maximum resistance force to insertion), 2 (insertion work), 5 (anterior-posterior force at rest), and 7 (maximum pressure at muscle contraction) before 60 years of age; we observed a disappearance of this effect with age (Figures 3, 5, and 7). However, the nulliparous trend line does not intersect the parous trend line for VTI parameters 3 (maximum stress-to-strain ratio), 6 (left-right force at rest), and 8 (muscle contraction force) before 60 years; we observed a disappearance of this effect with age. 3 of 8 parameters demonstrated a *P* value less than or equal to .05 for 2 subject subsamples divided by parity (non-parous vs parous; Table 1).

A limitation of this study is the relatively small sample (42 subjects). In addition, despite normal pelvic floor support (no prolapse), some analyzed subjects came to the urogynecologic office with some problematic conditions affecting the pelvic floor. Further research with a more representative sample will show more comprehensive distributions and peculiar features for normal values.

In conclusion, VTI allows biomechanical and functional characterization of pelvic floor conditions, which can be used for a better overall understanding of these conditions and a quantification of the deviation from normality. By adopting a standardized, objective functional assessment of the pelvis, more personalized treatments for pelvic floor conditions can be used. This holds numerous possibilities for clinical use, such as guiding surgical decision making (perhaps helping delineate which patients are candidates for an isolated repair vs a more global reconstructive procedure or whether a graft would be beneficial for a given defect), directing the use or region of application for energy-based therapies, directing physical therapy for muscle rehabilitation, or identifying areas of focus for patients with pelvic pain. The proposed approach can help further differentiate the types of vaginal conditions and understand how to tailor treatments for the individual patient for improved functional outcomes in the most effective manner.



**Corresponding Author:** Vladimir Egorov, PhD, Artann Laboratories, 1459 Lower Ferry Road, Trenton, NJ 08618, USA. Tel: 609 883-0100z; E-mail: [vegorov@artannlabs.com](mailto:vegorov@artannlabs.com)

*Conflicts of Interest:* V.E. is a co-founder and CEO of Advanced Tactile Imaging, Inc. H.vR. and N.S. are co-founders of Advanced Tactile Imaging, Inc. The other authors report no conflicts of interest.

*Funding:* Research reported in this publication was supported by the National Institute On Aging of the National Institutes of Health under Award Numbers R44AG034714 and SB1AG034714. The content is solely the responsibility of the authors and does not necessarily represent the official views of the National Institutes of Health.

## STATEMENT OF AUTHORSHIP

### Category 1

#### (a) Conception and Design

Vladimir Egorov; Miles Murphy; Vincent Lucente; Heather van Raalte

#### (b) Acquisition of Data

Miles Murphy; Vincent Lucente; Heather van Raalte; Sonya Ephrain; Nina Bhatia

#### (c) Analysis and Interpretation of Data

Vladimir Egorov; Miles Murphy; Vincent Lucente; Heather van Raalte; Sonya Ephrain; Nina Bhatia; Noun Sarvazyan

### Category 2

#### (a) Drafting the Article

Vladimir Egorov; Miles Murphy; Vincent Lucente; Heather van Raalte; Noun Sarvazyan

#### (b) Revising It for Intellectual Content

Vladimir Egorov; Miles Murphy; Vincent Lucente; Heather van Raalte; Sonya Ephrain; Nina Bhatia; Noun Sarvazyan

### Category 3

#### (a) Final Approval of the Completed Article

Vladimir Egorov; Miles Murphy; Vincent Lucente; Heather van Raalte; Sonya Ephrain; Nina Bhatia; Noun Sarvazyan

## REFERENCES

1. Goodman MP, Placik OJ, Matlock DL, et al. Evaluation of body image and sexual satisfaction in women undergoing female genital plastic/cosmetic surgery. *Aesthet Surg J* 2016; 36:1048-1057.
2. Filippini M, Del Duca E, Negosanti F, et al. Fractional CO2 laser: from skin rejuvenation to vulvo-vaginal reshaping. *Photomed Laser Surg* <https://doi.org/10.1089/pho.2016.4173>. E-pub ahead of print.
3. Shaw D, Lefebvre G, Bouchard C, et al. Female genital cosmetic surgery. *J Obstet Gynaecol Can* 2013;5:1108-1114.
4. Mirzabeigi MN, Jandali S, Mettel RK, et al. The nomenclature of "vaginal rejuvenation" and elective vulvovaginal plastic surgery. *Aesthet Surg J* 2011;31:723-724.
5. van Raalte H, Egorov V. Characterizing female pelvic floor conditions by tactile imaging. *Int Urogynecol J* 2015; 26:607-609; video supplement.
6. Sarvazyan A, Egorov V, Sarvazyan N. Tactile sensing and tactile imaging in detection of cancer. In: Harold KE, Rasooly A, eds. *Biosensors and molecular technologies for cancer diagnostics*. Abingdon, UK: Taylor & Francis; 2012. p. 337-352.
7. Duck FA. Physical properties of tissue: a comprehensive reference book. In: *Mechanical properties of tissue*. London, UK: Academic Press; 1990. p. 137-165.
8. Fung YC. *Biomechanics: mechanical properties of living tissues*. 2nd ed.; 1993.
9. Sarvazyan A. Elastic properties of soft tissues. In: Levy M, Bass HE, Stern RR, eds. *Elastic properties of soft tissues handbook of elastic properties of solids, liquids, and gases, Vol III*. New York: Academic Press; 2001. p. 107-127.
10. Timoshenko S, Goodier JN. *Theory of elasticity*. New York: McGraw-Hill Book Company; 1951.
11. Landau LD, Lipshitz EM. *Theory of elasticity*. 3rd ed.; 1970.
12. Taber AT. *Nonlinear theory of elasticity. Applications in biomechanics*. Singapore: World Scientific; 2004.
13. Egorov V, van Raalte H, Lucente V, et al. Biomechanical characterization of the pelvic floor using tactile imaging. In: Hoyte L, Damaser MS, eds. *Biomechanics of the female pelvic floor*. 1st ed. New York: Elsevier; 2016. p. 317-348.
14. van Raalte H, Lucente V, Egorov V. High definition pressure mapping of the pelvic floor muscles during Valsalva maneuver, voluntary muscle contraction and involuntary relaxation. *Female Pelvic Med Reconstr Surg* 2015;21:S149-S150.
15. DeLancey JO. Pelvic floor anatomy and pathology. In: Hoyte L, Damaser MS, eds. *Biomechanics of the female pelvic floor*. 1st ed. New York: Elsevier; 2016. p. 13-51.
16. Dietz HP. *Pelvic floor ultrasound. Atlas and text book*. Springwood, Australia: Creative Commons Attribution License; 2016.
17. Petros P. *The female pelvic floor: function, dysfunction and management according to the integral theory*. 3rd ed. Berlin: Springer; 2010.
18. van Raalte H, Lucente V, Ephrain S, et al. Intra- and inter-observer reproducibility of vaginal tactile imaging. Presented at: 37th Annual Meeting of the American Urogynecologic Society; Denver, CO; September 27–October 1, 2016.
19. Egorov V, Sarvazyan AP. Mechanical imaging of the breast. *IEEE Trans Med Imaging* 2008;27:1275-1287.
20. van Raalte, Bhatia N, Egorov V. Is it all just smoke and mirrors?: Vaginal laser therapy and its assessment by tactile imaging. *Int Urogynecol J* 2016;(Suppl. 1):S120-S121.
21. van Raalte H, Lucente V, Ephrain S, et al. Pelvic organ prolapse surgery characterization by vaginal tactile imaging. *Int Urogynecol J* 2016;(Suppl 1):S117-S118.
22. van Raalte H, Egorov V. Tactile imaging markers to characterize female pelvic floor conditions. *Open J Obstet Gynecol* 2015;5:505-515.

23. van Raalte H, Egorov V, Lucente V, et al. 3D tactile imaging in early prolapse detection. *Neurorol Urodyn* 2013; 32:704-705.
24. Egorov V, van Raalte H, Lucente V. Quantifying vaginal tissue elasticity under normal and prolapse conditions by tactile imaging. *Int Urogynecol J* 2012;23:459-466.
25. van Raalte H, Lucente V, Egorov V. 3-D imaging and quantifying vaginal tissue elasticity under normal and prolapse conditions. *Int Urogynecol J* 2011;22(Suppl. 1): S183-S184.
26. Egorov V, van Raalte H, Sarvazyan A. Vaginal tactile imaging. *IEEE Trans Biomed Engin* 2010;57:1736-1744.
27. Ranstam J. Multiple P-values and Bonferroni correction. *Osteoarthritis Cartilage* 2016;24:763-764.
28. Perneger TV. What's wrong with Bonferroni adjustments. *BMJ* 1998;316:1236-1238.
29. Chantereau P, Brieu M, Kammal M, et al. Mechanical properties of pelvic soft tissue of young women and impact of aging. *Int Urogynecol J* 2014;25:1547-1553.
30. Murad-Regadas SM, Regadas FS, Rodrigues LV, et al. Influence of age, mode of delivery and parity on the prevalence of posterior pelvic floor dysfunctions. *Arq Gastroenterol* 2011; 48:265-269.
31. Slieker-ten Hove MC, Pool-Goudzwaard AL, Eijkemans MJ, et al. Pelvic floor muscle function in a general female population in relation with age and parity and the relation between voluntary and involuntary contractions of the pelvic floor musculature. *Int Urogynecol J Pelvic Floor Dysfunct* 2009; 20:1497-1504.